

RI-Mode confinement and performances on TEXTOR-94 under siliconized wall conditions

A.M.MESSIAEN¹, J.ONGENA¹§, B.UNTERBERG², P.DUMORTIER¹, G.FUCHS²,
R.JASPERS³, H.R.KOSLOWSKI², A.KRAEMER-FLECKEN², G.MANK², J.RAPP²,
G.VAN WASSENHOVE¹, R.R.WEYNANTS¹ and TEXTOR-94 TEAM^{1,2,3}

Trilateral Euregio Cluster

(1) *Laboratoire de Physique des Plasmas - Laboratorium voor Plasmafysica, Association "EURATOM-Belgian State"*

Ecole Royale Militaire- B-1000 Brussels - Koninklijke Militaire School

(2) *Institut für Plasmaphysik, Forschungszentrum Jülich GmbH
Association "Euratom-KFA", D-52425 Jülich, FRG*

(3) *FOM Instituut voor Plasmafysica 'Rijnhuizen'
Association "EURATOM-FOM"*

P.O.Box 1207, 3430 BE Nieuwegein, The Netherlands.

1. Introduction.

The interest and main characteristics of the RI-mode regime of TEXTOR-94 (limiter machine with circular cross-section) have been discussed in references [1,2,3]. The transition to the RI-mode is usually obtained by injecting neon or argon under boronized wall conditions in an L-mode plasma of sufficiently large density and heated at least partially by co-injection. The radiating belt can also be obtained from the sputtering of silicon under siliconized wall conditions as seen in Fig.1b [4]. In this case, for a deuterium plasma and given operational conditions, the radiated power fraction $\gamma = P_{\text{rad}}/P_{\text{tot}}$ (where P_{rad} is the radiated power and P_{tot} the total heating power) is nearly independent of the density but its value decreases with the age of the silicon layer which is progressively changes to a mixture of silicon and carbon. Edge radiation cooling is maintained during the complete discharge with a roughly constant value of γ . In this case an abrupt transition to another confinement regime is not observed and high performance RI-mode conditions can be simply obtained by rising the density through appropriate gas puff. This paper summarizes the properties and performances of the RI-mode obtained with a freshly siliconized wall.

2. Main characteristics of the RI-mode due to silicon sputtering.

Confinement. Fig. 1a shows the time evolution of the diamagnetic energy E_{dia} , the central line averaged density \bar{n}_{e0} and P_{tot} for a discharge heated by NB co-injection and ICRH as indicated on the figure. This discharge is performed about 50 discharges after the siliconization implementation. The plasma energy as expected from the L-mode scaling ITER L89-P and from the ELM-free H-mode scaling ITER H93-P is also shown. The figure illustrates that as result of the density rise (which is pre-programmed as also shown in the figure) the plasma energy increases from the L-mode to the ELM-free H-mode level.

In reference [3,5] it was shown that the RI-mode with its linear density dependence is the counterpart with additional heating of the linear ohmic confinement (LOC) whereas the L-mode is the counterpart of the Saturated Ohmic confinement (SOC). The energy confinement time scaling of the RI-mode and of the LOC can be described by the same law

$$\tau_{\text{RI}} = K \bar{n}_{e0} (P_{\text{tot}})^{-2/3} \quad (1)$$

where K is a constant (the dependence on the toroidal magnetic field Bt is found negligible). The confinement behaviour of the RI-L.O.C. mode and of the L-S.O.C. mode can be conveniently displayed in the diagram introduced in Ref.[3] showing the normalized confinement time $\tau_{\text{E}}(P_{\text{tot}})^{2/3}/I_p$ versus the Greenwald number $\bar{n}_{e0}/n_{\text{GR}}$ (I_p is the plasma current and n_{GR} is the Greenwald density limit and we use as units s, MW, MA, 10^{20}m^{-3}). The experimental data of freshly siliconized discharges heated by NB co-injection and a possible assist of ICRH are

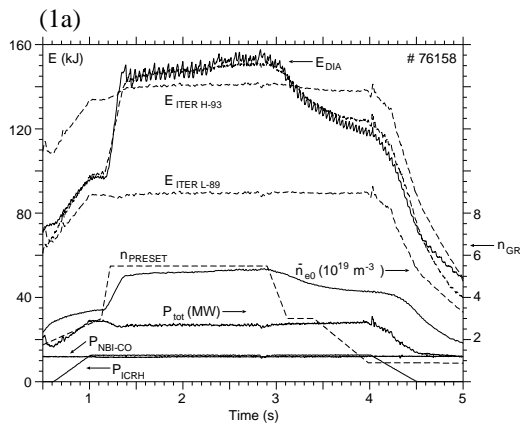


Fig.1a) Time evolution of E_{dia} , \bar{n}_{e0} , P_{tot} , P_{nbi-co} and P_{ICRH} for a RI-mode discharge with siliconized wall. The dashed lines show the predictions of the ITER L89, ITER H93 and RI (from Eq.(1) with $K=0.2$) scalings and also the preset value for \bar{n}_{e0} . ($I_p=0.4MA$, $B_t=2.25T$).

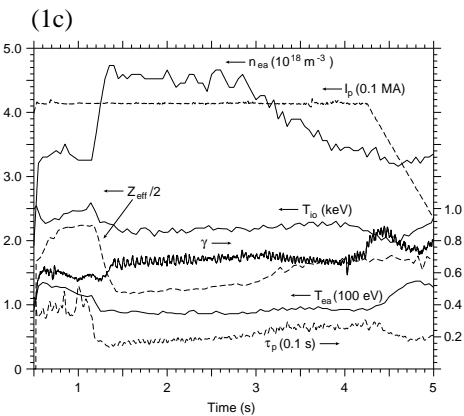
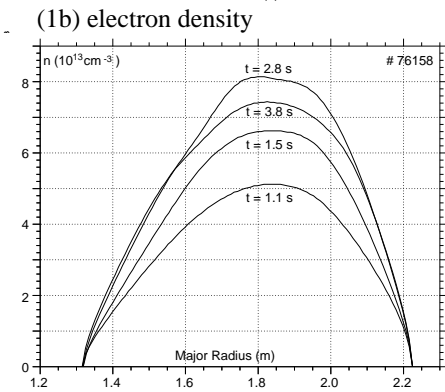


Fig.1c) Time evolution of n_{ea} , T_{ea} , $T_e(0)$, τ_p , γ , central Z_{eff} and I_p (n_{ea} and T_{ea} are taken from the similar discharge #76156).

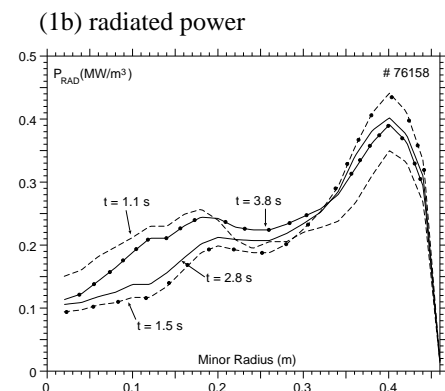
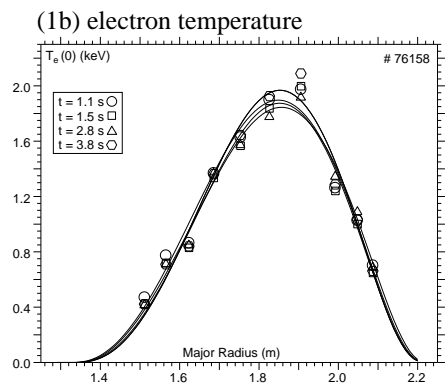


Fig.1b) Radial profiles of electron density and temperature and of radiated power density for selected times.

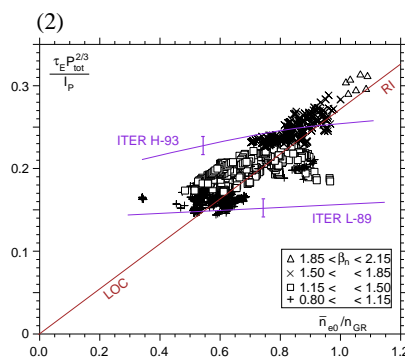


Fig.2 Normalized diagram of τ_E versus \bar{n}_{e0} for data obtained with freshly siliconized wall. A comparison is given with the predictions of L, H, and RI-Mode (from Eq.(1) with $K=0.18$) scalings.

displayed in such a diagram in Fig.2 together with the scaling given by Eq.(1) (LOC-RI straight line) and the predictions of the ITER L-89 and ITER H-93 scaling law. The error bars added to the two last laws indicate the scatter of the predictions in the normalized diagram for the range of P_{tot} ,

I_p and \bar{n}_{e0} of the data set. The value $K=0.18$ of Eq.(1) is the one chosen in [3] to describe the neon and argon seeded RI-mode and the ohmic LOC discharges. The experimental points are nicely following the linear increase with the density for densities in excess of the one corresponding to the crossing between the L-mode and the RI-mode laws ($\bar{n}_{e0} \cong 0.55 n_{GR}$). In addition, most of the points lie somewhat above the scaling established for the RI-mode with boronized wall and the best points would need a 10-15% larger proportionality factor K than the value used for the neon-argon database. At lower density the global confinement time τ_E follows with some improvement the L-mode scaling and does not retain the linear density dependence. The energy evolution of the discharge shown in Fig.1a changes in close agreement with Eq.(1) for the whole duration of the discharge with a constant $K=0.2$ (see the dotted line which mimics accurately E_{dia}). ELM-free H-mode confinement quality is obtained for $\bar{n}_{e0}/n_{GR}=0.8-0.85$.

The confinement improvement is interpreted by the reduction of ITG micro-instabilities resulting mainly from the peaked density profile and the presence of the radiating impurity [3,6]. The density peaking factor $\gamma_n = n_e(0)/\langle n_e \rangle$ remains for the whole duration of the discharge higher than for an L-mode discharge with the same operating parameters.

Temperature. The scaling (1) implies that the mean temperature of the discharge $\langle T \rangle$ is proportional to $(P_{tot})^{1/3}$ and is independent of \bar{n}_{e0} . This is very well verified on Fig.1b which displays for selected times during the density ramp the radial density and electron temperature profiles. The T_e bulk profiles remain practically unchanged. The central ion temperature also does not vary much as also illustrated in Figs. 1c and 3.

Beta. From Eq.(1), one obtains as scaling for the normalized beta $\beta_n = 15.9K(\bar{n}_{e0}/n_{GR})(P_{tot})^{1/3}/B_t$, showing that β_n is depending mainly on the Greenwald number and only weakly on the power. This is illustrated in Fig. 2 where β_n increases continuously with the density although the variation in power is large ($1.4 < P_{tot} < 3.2$ MW). Figure 3 shows a discharge going to the experimental limit of $\beta_n = 2-2.2$ as a result of the density rise by gas puff. The limit of β_n is generally associated with an increase of the density peaking factor (see Fig.3) and with the onset of MHD activity which leads to an energy rollover, possibly followed by minor or hard disruptions [7].

Effective charge. The central value of Z_{eff} is mainly due to silicon and is large at low density but decreases strongly with the rise of the density as shown in Fig.1c. Under performing RI-mode conditions ($f_{H93} \cong 1$, $\bar{n}_{e0}/n_{GR} \cong 1$) $Z_{eff} = 2-2.5$ as for the neon seeded RI-mode discharges [13].

Neutron yield. Is mainly due to beam-target reactions which depend on the central dilution and electron temperature. The neutron increase appearing with the density rise (see Fig.3) is attributed to the decrease of the dilution and the increase of the thermal production.

Edge parameters and particle confinement time τ_p . When \bar{n}_{e0} rises the edge electron temperature T_{ea} decreases and the edge density n_{ea} increases as shown in Fig.1c. This results in a reduction of the penetration depth of the neutrals and a reduction of τ_p [12] as also shown in Fig.1c. The effect of a too large reduction of τ_p is discussed in the next section.

3. Conditions of existence of the RI-mode regime.

Various operational conditions have to be fulfilled to obtain the RI-mode regime with the above-mentioned full performances :

(i) Isotopic effects. 1) In a H plasma with freshly siliconized wall a reduced sputtering of silicon by H as compared to D leads to lower values of γ than for a D discharge. Therefore addition of neon is

required to obtain an RI-mode regime, but with confinement and β_n reduced in proportion to $\approx\sqrt{A_I} = \sqrt{2}$ as for L-mode. 2) In a D plasma D injection is required to obtain optimum performance [9,10].

(ii) *Heating scenario*. Heating with at least $\approx 20\%$ of co-injection is required [11].

(iii) *Fueling and recycling*. Too strong gas puff leads to confinement saturation followed by a decrease towards L-mode scaling (see lower points in Fig.2). The maximum gas puff rate that the RI-mode can sustain decreases with the age of the silicon layer, i.e. with the obtained value for γ . As a result, the maximum density at which the RI-mode is observed is then no longer imposed by a β_n limit but by a limit of edge gas flux or too low a value of τ_p as illustrated in Fig.4: at 1.1s the preset value of the density is increased and the D gas valve is opened; after an initial rise, the energy confinement (as indicated by f_{H93}) decays and does not follow the RI-mode scaling indicated by the dotted line. A recovery of the RI-mode scaling and of its full performance is nevertheless possible by seeding of neon (starting at 1.6s). This seeding leads to an increase of τ_p and of the fueling efficiency which results in the closure of the D gas valve. Figure 4 also shows that this allows to recover a larger γ_n , high confinement and higher neutron yield. The aging of the silicon layer can thus be compensated by neon seeding. Like for neon seeded discharges the horizontal position of the plasma is a critical parameter for optimal performance. It is thought that this positioning affects the confinement through its influence on the gas throughput [8]. The link between fueling, recycling, density peaking and confinement improvement is under investigation [8,12].

References

[1] A. Messiaen et al., Phys. Rev. Lett., **77**(1996)825.
 [2] A. Messiaen et al., Phys. Plasmas, **4**(1997)1690.
 [3] R. Weynants et al., Proc.17th IAEA Conf. Yokohama (1998), paper IAEA-CN-69/EX1/3; Nucl. Fusion, to be published (1999)
 [4] U.Samm et al., J.Nucl. Mat. **220-222**(1995)25.
 [5] A. Messiaen et al., Comments Plasma Phys. Contr. Fusion, **18**(1997)221.
 [6] M. Tokar' et al., Invited paper, this conference.
 [7] H. R. Koslowski et al., this conference.
 [8] B. Unterberg et al., J. Nucl. Mat. **266-269**(1999)75
 [9] A. Messiaen et al., Proc. 1998 ICPP & 25th EPS CCFPP, Prague, Eur. Conf. Abs. Vol22C,568
 [10] J. Ongena et al., this conference.
 [11] A. Messiaen et al., Radio Freq. Power in Plasmas (12th Top. Conf. Savannah 1997) AIP Conf. Proc. **403**, p.41
 [12] B. Unterberg et al., this conference.
 [13] R.Jaspers et al., this conference.

§Researcher at FWO Vlaanderen

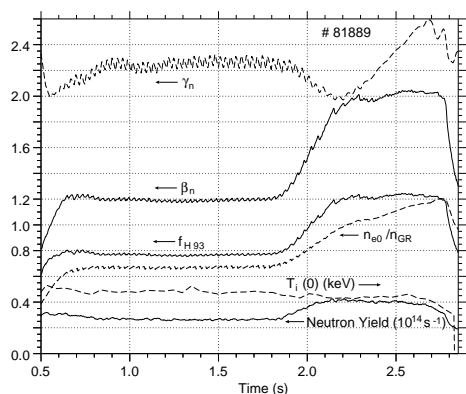


Fig.3 Time evolution of β_n , f_{H93} (enhancement factor with respect to ITER H93 scaling), \bar{n}_{e0}/n_{GR} , $T_i(0)$, neutron yield, and γ_n for a siliconized wall discharge reaching the β limit. ($I_p=0.4MA$, $B_t = 2.25T$).

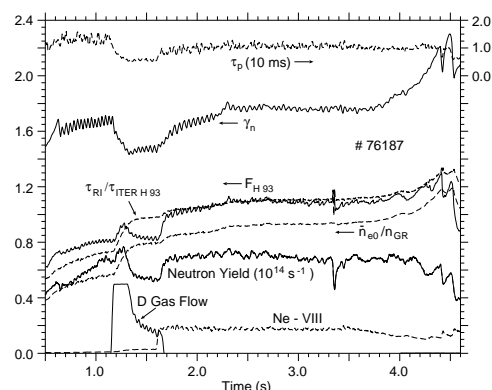


Fig.4 Time evolution of f_{H93} (compared with values predicted from Eq.(1)), neutron yield, \bar{n}_{e0}/n_{GR} , $T_i(0)$, τ_p and γ_n for a discharge with a siliconized wall, with additional Ne seeding. The D gas puff rate and brilliance of NeVIII are also shown. ($I_p=0.4MA$, $B_t=2.25T$).